THE JOURNAL OF PHYSICAL CHEMISTRY A
A JOURNAL OF THE AMERICAN CHEMICAL SOCIETY

pubs.acs.org/JPCA

Article

Spectroscopic Characterization of Highly Excited Neutral Chromium Tricarbonyl

Published as part of The Journal of Physical Chemistry A virtual special issue "Alec Wodtke Festschrift".

Tiantong Wang, Zhaoyan Zhang, Wenhui Yan, Shuai Jiang, Shangdong Li, Jianxing Zhuang, Hua Xie, Gang Li,* and Ling Jiang*

Cite This: *J. Phys. Chem. A* 2024, 128, 3321−3328

Read Online

ACCESS | Metrics & More | Article Recommendations | Supporting Information

ABSTRACT: Spectroscopic characterization of highly excited neutral transition-metal complexes is important for understanding the multifaceted reaction mechanisms between metals and ligands. In this work, the reactions of neutral chromium atoms with carbon monoxide were probed by size-specific infrared spectroscopy. Interestingly, $Cr(CO)_3$ was found to have an unprecedented $^7A_2''$ septet excited state rather than the singlet ground state. A combination of experiment and theory shows that the gas-phase formation of this highly excited $Cr(CO)_3$ is facile both thermodynamically and kinetically. Electronic structure and bonding analyses indicate that the valence electrons of Cr atoms in the septet $Cr(CO)_3$ are in a relatively stable configuration, which facilitate the highly excited structure and the planar geometric shape (D_{3h} symmetry). The observed septet $Cr(CO)_3$ affords a paradigm for exploring the structure, properties, and formation mechanism of a large variety of excited neutral compounds.

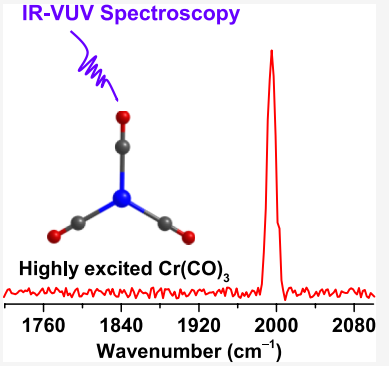

1. INTRODUCTION

Transition-metal complexes (TMCs) are a very rich class of compounds with a wide range of application prospects.[1−6] Electronically excited TMCs are usually more reactive and are vital intermediates in photoinduced reactions, such as solar energy conversion,[7,8] photocatalytic hydrogen production,[9,10] selective carbon−hydrogen bond activation,[11,12] etc. Therefore, the investigation of excited intermediates in the complicated processes at the molecular level is crucial to understanding the fundamental reaction mechanisms. The electronic structures, excited-state lifetime, and electron excitation dynamics of excited TMCs have been explored by X-ray spectroscopy [i.e., time-resolved resonance inelastic X-ray spectroscopy[13,14] and X-ray absorption spectroscopy (XAS)[15,16]]. For instance, the orbital-resolved XAS spectroscopy of $CpRh(CO)_2$(octane) reveals that the Rh → C−H backdonation in the octane group is enhanced by X-ray excitation of the 2p electron to the 4d orbital in the Rh atom, resulting in the efficient C−H activation.[12] The bonding scheme of TM carbonyls is generally regarded as a synergy of the CO → TM σ donation and CO ← TM π backdonation and the vibration frequency of the CO ligand is sensitive to the electronic structure of the metal atom.[17−19] The excited TM carbonyls have been inspected by time-resolved vibration spectroscopy.[20−24] For example, the excited-state photoproduct $^3Fe(CO)_4$ exhibits a higher reactivity than the ground-state photoproduct $^1Fe(CO)_4$ toward the reaction with the solvent ligands.[24]

The chromium carbonyl complexes $Cr(CO)_n$ are one of the fundamental metal carbonyl species, which are widely used in aromatic activation,[25−27] asymmetric catalysis,[28−30] olefin polymerization,[31] and other processes. For instance, the $Cr(CO)_3$ unit could tune the chemical properties of arene in (η^6-arene)$Cr(CO)_3$ via the electron-withdrawing effect, resulting in the activation of arene.[25−27,32] Experimental [i.e., matrix isolation infrared (IR) spectroscopy and time-resolved transient IR spectroscopy] and theoretical studies have identified a series of ground-state neutral chromium carbonyls $Cr(CO)_n$ (n = 1−6).[18,33−38] The charged chromium carbonyls with ground states have also been extensively investigated by IR photodissociation spectroscopy, electron spin resonance spectroscopy, and photoelectron spectroscopy.[39,40] Much efforts have been made to study the structure of $Cr(CO)_3$ as a fundamental simple metal carbonyl species. The methane-matrix IR spectrum of $Mo(CO)_3$ was shown to include a symmetric (1981 cm^{-1}) and an antisymmetric (1862 cm^{-1}) CO stretching mode, indicative of a C_{3v} structure verified by partial substitution with ^{13}CO.[34] $Cr(CO)_3$ and $Mo(CO)_3$ were shown to have an analogous pattern of symmetric and

Received: February 20, 2024
Revised: March 25, 2024
Accepted: April 9, 2024
Published: April 18, 2024

https://doi.org/10.1021/acs.jpca.4c01120
J. Phys. Chem. A 2024, 128, 3321−3328

antisymmetric CO stretching modes in the methane matrix and were concluded to have the same structure.[34] Methane-matrix IR spectroscopy of $Cr(CO)_3$ yields the symmetric and antisymmetric CO vibration frequencies at 1979 and 1859 cm^{-1}, respectively.[34] The antisymmetric CO stretch of gas-phase $Cr(CO)_3$ was measured at 1880 cm^{-1} by transient IR absorption spectroscopy.[33] Along with theoretical calculations,[36,38] the ground state of $Cr(CO)_3$ was characterized to have a C_{3v} pyramidal structure with an $^1A_1$ electronic state.

Thus far, spectroscopic characterization of chromium carbonyls with an excited state remains elusive. Here, neutral chromium carbonyls were prepared in a laser-vaporization cluster source in the gas phase and characterized by using IR-vacuum ultraviolet (IR-VUV) spectroscopy, which could provide the spectral characteristics of size-specific clusters without interference from other species. Experimental spectra in conjunction with quantum chemical calculations reveal that $Cr(CO)_3$ has an intriguing $^7A_2''$ septet highly excited state rather than the singlet ground state, evidencing a special electronic structure and unique reaction kinetics during the formation of serial chromium carbonyl complexes.

2. EXPERIMENTAL AND THEORETICAL METHODS

The IR-VUV apparatus[41−43] was utilized for the present experiments. The ablated chromium atoms reacted with pulsed CO (99.99%). The IR-VUV depletion scheme was used to measure the IR spectra of neutral chromium carbonyls, for which the vibrational excitation was attained by a tunable IR laser (LaserVision) and ionization detection was accomplished by a 193 nm VUV laser (EX5*A*/500, Gamlaser) with a delay of approximately 50 ns. The OPO/OPA system was operated in the mid-IR region of 1500−2300 cm^{-1}, with a line width of 1 cm^{-1} and a pulse energy of 2 mJ. The calibration of IR wavelength was done by using a wavelength meter (High-Finesse GmbH, WS6-200 VIS IR). While the repetition rates of the pulse valve, 532 nm laser, and 193 nm laser were 20 Hz, that of the IR laser was 10 Hz. A difference spectrum (IR laser OFF minus IR laser ON) was thus acquired, which was typically done with 1800 laser shots and 2 cm^{-1} steps at every IR wavelength.

Theoretical calculations of the present systems were fulfilled at the B2PLYP-D3/def2-TZVPP level of theory by using Gaussian 16.[44] The calculated IR frequencies were scaled by a factor of 0.991 that was determined by the calculated/experimental (2143 cm^{-1}) ratio of the stretching mode of a free CO molecule (2002/2143 cm^{-1} = 0.991) and were convoluted with a Gaussian function (fwhm = 10 cm^{-1}). The bonding nature in $Cr(CO)_3$ was analyzed with energy decomposition analysis with natural orbitals for the chemical valence (EDA-NOCV) method at the B3LYP-D3(BJ)/TZ2P level by using the ADF 2023.104 program package.[45,46] In EDA-NOCV analysis, the intrinsic interaction energy (ΔE_{int}) between two fragments was decomposed into an electrostatic interaction term (ΔE_{elstat}), Pauli repulsion interaction term (ΔE_{Pauli}), orbital interaction term (ΔE_{orb}), and dispersion energy correction term (ΔE_{disp}).[47] The electron localization function (ELF) was calculated at the B2PLYP-D3/def2-TZVPP level with Multiwfn software.[48−50]

3. RESULTS AND DISCUSSION

The experimental IR spectrum of $Cr(CO)_3$ is shown in Figure 1a. A single peak was observed at 1995 cm^{-1}, with a maximum depletion ratio of 43.4%. The observation of only one band in the present C−O stretching spectrum of $Cr(CO)_3$ indicates that the structure of this complex has a very high symmetry. In order to understand the experimental spectrum and identify its molecular structure, we performed quantum chemical calculations at the B2PLYP-D3/def2-TZVPP level. The molecular structures, relative energies, and IR spectra of $Cr(CO)_3$ with different electronic states are shown in Figure S1. The corresponding calculated peak positions, intensities, and vibration modes are listed in Table S1.

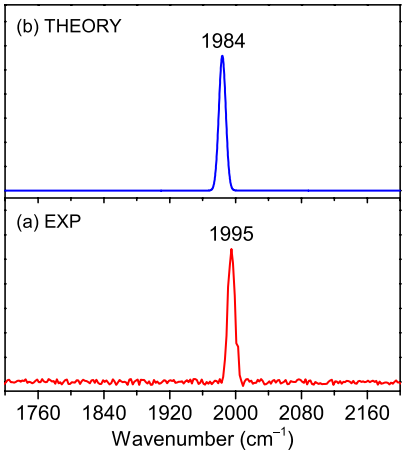

Figure 1. IR-VUV spectrum of the neutral $Cr(CO)_3$ complex (a) and calculated IR spectrum of $Cr(CO)_3$ with the $^7A_2''$ electronic state (b).

$Cr(CO)_3$ has an $^1A_1$ ground electronic state with a C_{3v} symmetry, which is consistent with previous investigations.[33,35−38] Two CO stretching absorption peaks attributed to E and A_1 vibration modes are predicted at 1875 and 1970 cm^{-1}, respectively. The calculated peaks of ground-state $Cr(CO)_3$ are in good agreement with previous experimental ones at 1859 and 1979 cm^{-1} observed in the methane matrix,[34] which confirms our strategy of the present computational method. However, the calculated IR spectrum of singlet $Cr(CO)_3$ (Figure S1b) is very different from the present experimental spectrum (Figure S1a), implying the presence of a new electronic state.

The $Cr(CO)_3$ complex with an electronically excited state of $^3B_1$ is predicted to have C_{2v} symmetry, which lies higher in energy by 25.8 kcal/mol than that of the ground state. The calculated C−O stretching vibrational spectrum of this triplet $Cr(CO)_3$ consists of two intense peaks at 1997 and 2051 cm^{-1} (Figure S1c), which do not agree with the experimental spectrum (Figure S1a). The $Cr(CO)_3$ complex with a $^5B_2$ state lies higher in energy by 19.3 kcal/mol than the ground state. Three C−O stretching absorption peaks of this quintet $Cr(CO)_3$ are predicted at 1950, 2000, and 2081 cm^{-1}, corresponding to the B_2, A_1, and A_1 stretching vibration modes, respectively. The $^5B_2$ electronic state of $Cr(CO)_3$ can be ruled out by the discrepancy of its calculated positions and the number of absorption peaks (Figure S1d) from the experimental spectrum (Figure S1a). The $Cr(CO)_3$ complex with an $^7A_2''$ electronic state is predicted to have D_{3h} symmetry, which lies 24.6 kcal/mol above the ground state. The calculated C−O stretching vibrational spectrum of this septet $Cr(CO)_3$ consists of a single peak at 1984 cm^{-1}, which is attributed to the doubly degenerate antisymmetric stretching vibration mode and matches the observed spectral feature (1995 cm^{-1}). The concert between the simulated IR spectrum

https://doi.org/10.1021/acs.jpca.4c01120
J. Phys. Chem. A 2024, 128, 3321−3328

of septet $Cr(CO)_3$ and the experimental one (Figure 1) is rational to reinforce that the observed $Cr(CO)_3$ has an electronically excited state. As shown in Figure 2, the increase

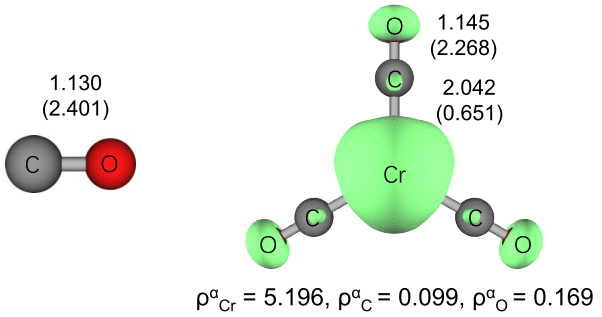

Figure 2. Optimized structures of CO and $^7A_2''$ $Cr(CO)_3$. Bond lengths (Å) and Mayer bond orders are given in regular font and in parentheses, respectively. The isosurface value of spin density of $Cr(CO)_3$ is set to 0.01. The spin populations of each atom in $Cr(CO)_3$ are also given.

of bond length and the decrease of bond order of the CO group in $Cr(CO)_3$ as compared to the free CO support the red shift of the C−O stretching vibration frequency, indicative of CO activation by the chromium atom.

The observation of highly excited chromium tricarbonyl is quite surprising because the ground-state complex is generally identified in the laser-vaporization supersonic expansion source.[40,51] Since the reactions under the laser-vaporization plasma conditions are too complicated to be clearly characterized, the possible formation mechanisms of septet $Cr(CO)_3$ were explored by quantum chemical calculations. The formation energies of $Cr(CO)_n$ (n = 1−3) initialed from the ground-state chromium atom are listed in Table S2. Our calculations indicate that Cr(CO) has an $^7A'$ ground electronic state, which is consistent with previous theoretical and experimental results.[35,36,52] The Cr (^7S) + CO ($^1\Sigma^+$) → Cr(CO) ($^7A'$) reaction is exothermic with a predicted value of 3.9 kcal/mol at the B2PLYP-D3/def2-TZVPP level of theory (Table S2). $Cr(CO)_2$ is calculated to have a $^7\Pi_u$ ground state, consistent with the single-reference ab initio MP2 and CCSD(T) calculations.[36] The multireference ab initio (MS-)CASPT2 calculations of $Cr(CO)_2$ indicated that the $^5\Pi_g$ and $^7\Pi_u$ states were nearly degenerate, in which the absorption peak of 1914 cm^{-1} in the matrix-isolation and transient absorption spectra was attributed to the $^7\Pi_u$ electronic state.[38] Thus, it is reasonable to confirm the presence of $Cr(CO)_2$ ($^7\Pi_u$) in the reaction products. The Cr(CO) ($^7A'$) + CO ($^1\Sigma^+$) → $Cr(CO)_2$ ($^7\Pi_u$) process is exothermic with a predicted value of 15.5 kcal/mol (Table S2). $Cr(CO)_2$ ($^7\Pi_u$) reacts with CO to produce $Cr(CO)_3$ ($^7A_2''$), which is exothermic by 21.2 kcal/mol without spin change and is thermodynamically and kinetically feasible.

There is one possibility that low states of $Cr(CO)_3$, which could exist in the experiment, are too stable to dissociate under the present condition. For instance, the dissociation energy of the singlet $Cr(CO)_3$ to a singlet $Cr(CO)_2$ and a singlet CO is calculated to be 59.3 kcal/mol. The dissociation of internally cold singlet $Cr(CO)_3$ needs at least ten IR photons at ∼2000 cm^{-1}. The low-energy IR laser beam delivered from the tabletop LaserVision system is thus not sufficient to dissociate singlet $Cr(CO)_3$.

While both experimental and theoretical studies indicate that $Cr(CO)_3$ has an $^1A_1$ electronic ground state, the de-excitation process of electronically excited $Cr(CO)_3$ would happen via nonradiative or radiative transition.[53−55] Considering that the molecules travel in a high vacuum (<10^{-5} Pa) after leaving the laser-vaporization cluster source, the de-excitation efficiency

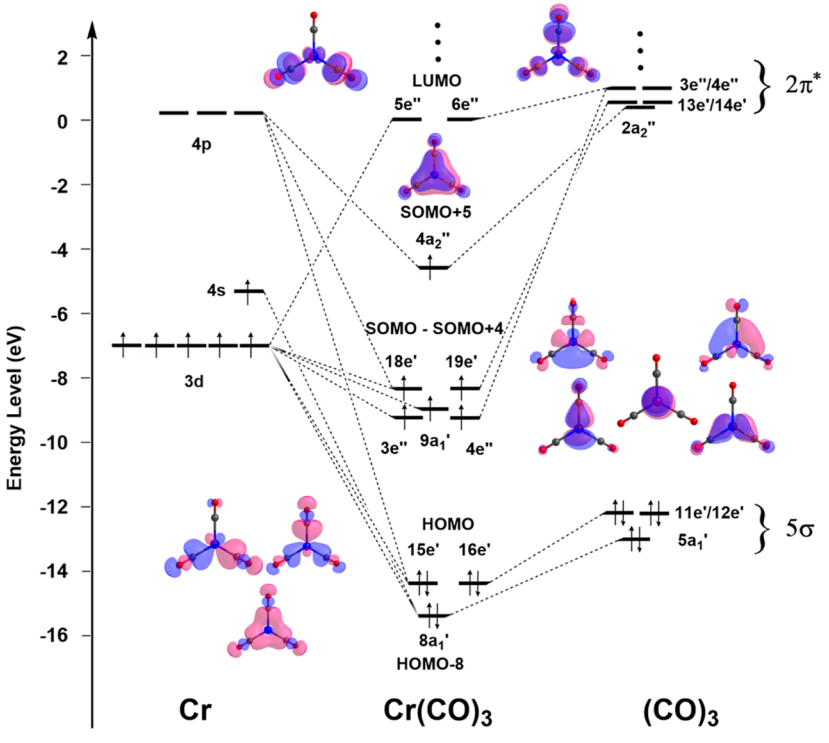

Figure 3. B2PLYP-D3/def2-TZVPP bonding scheme of septet $Cr(CO)_3$.

https://doi.org/10.1021/acs.jpca.4c01120
J. Phys. Chem. A 2024, 128, 3321−3328

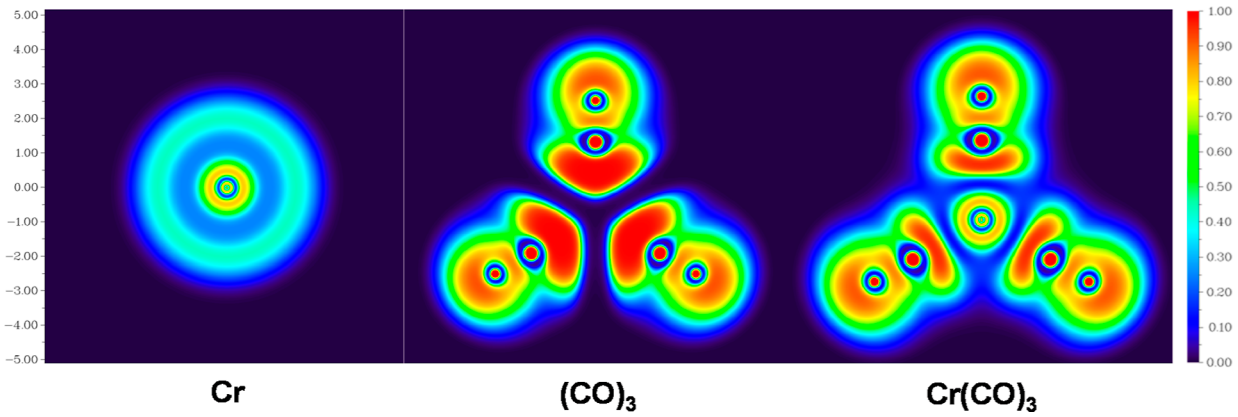

Figure 4. B2PLYP-D3/def2-TZVPP ELF maps of the Cr atom, $(CO)_3$ group, and septet $Cr(CO)_3$.

caused by nonradiative transitions in this system may be very weak. The radiative de-excitation transition between different electron multiplicities is a spin-forbidden process owing to the spin−orbit coupling with small transition probability and a time scale ranging from microseconds to several seconds.[56−58] In our experiments, the neutral clusters stay in a high vacuum for at least 200 μs before ionization,[41] and the electronically excited $Cr(CO)_3$ cannot be fully de-excited to the ground state in this time range and can therefore be detected. It can also be inferred that the lifetime of the septet $Cr(CO)_3$ complex may be longer than 200 μs in the gas phase. The determination of the precise lifetime of septet $Cr(CO)_3$ needs further experimental and theoretical studies of excited dynamics.

A series of bonding analyses were performed to comprehend the electronic structure of the $Cr(CO)_3$ ($^7A_2''$) complex. Natural bond orbital analysis shows that the coefficient of the Cr atom in the Cr−C bond is 17.66% with a contribution of s(32.05%) p(63.47%) d(4.47%), indicating that the Cr atom undergoes a sp^2 hybridization with benefit for the D_{3h} symmetry. Energy levels and 3D isosurfaces of the most important bonding orbitals of the $Cr(CO)_3$ ($^7A_2''$) complex are shown in Figure 3, and the contributions of atomic orbitals (AOs) to molecular orbitals (MOs) are given in Table S3. The 3d, 4s, and 4p AOs of the Cr atom and the 5σ and 2π* MOs of $(CO)_3$ together construct the valence MOs of $Cr(CO)_3$. The two lowest unoccupied MOs (LUMOs, 5e″ and 6e″) are doubly degenerate π-type antibonding orbitals formed between the 3d AOs and the 2π* MOs of $(CO)_3$. The highest single occupied MO (SOMO+5, $4a_2''$) is a π-type bonding orbital between the $4p_z$ AO of the Cr atom and $2a_2''$ MOs of $(CO)_3$. SOMO to SOMO+4 mainly consists of Cr d orbitals. The SOMO+3 (18e′) and SOMO+4 (19e′) are doubly degenerate orbitals, including the backdonation of Cr 3d AOs to the $\pi^*_\perp$ MOs of CO groups. The SOMO+2 ($9a_1'$) orbital is a nonbonding orbital, mainly the $3d_{z^2}$ orbitals of the Cr atom, and also contains a small part of the 4s orbital component. The SOMO (3e″) and SOMO+1 (4e″) are also doubly degenerate orbitals containing the backdonation of Cr 3d AOs to the $\pi^*_\parallel$ MOs of CO groups. The two highest occupied MOs (HOMOs, 15e′ and 16e′) are doubly degenerate σ-bonding orbitals, with the main contribution from the donation of CO 5σ orbitals to the Cr 4p orbitals. The HOMO−8 ($8a_1'$) is also a σ-bonding orbital, coming from the interaction between the CO 5σ orbital and the Cr 4s orbital. According to the orbital analysis, the single electrons are mainly located at the Cr atom, which agrees well with the spin population of $\rho_{Cr}{}^{\alpha} = 5.196$, $\rho_C{}^{\alpha} = 0.099$, and $\rho_O{}^{\alpha} = 0.169$. It can be seen that a π-type orbital ($4a_2''$) hosts a single electron, resulting in the distribution of electron spins on the C and O atoms, which is consistent with the shape of spin density as shown in Figure 2.

To visualize the electron distributions and bonding features, we calculated the ELF of Cr, $(CO)_3$, and $Cr(CO)_3$ ($^7A_2''$) (Figure 4). For the Cr atoms, the K-shell and L-shell (principal quantum number = 1 and 2) electrons remain spherical when forming the $Cr(CO)_3$ complex, showing the inertia of the inner-shell electrons. The M-shell (principal quantum number = 3) electrons have slight deformation in the D_{3h} field, showing few bonding interactions with the CO groups. The N-shell (principal quantum number = 4) electrons of the ground-state Cr atom are located in the region of 2.0 Å away from the nucleus, but it is not clearly shown in the ELF map of $Cr(CO)_3$, because the N-shell electrons of the Cr atom are mainly localized between Cr and C due to bonding. The localization regions of the CO lone-pair electrons shrink after the formation of $Cr(CO)_3$. The attractors between Cr and C indicate that the Cr−C bonds feature obvious covalent-bond characteristics.

The EDA-NOCV results of the $Cr(CO)_3$ ($^7A_2''$) complex are given in Table 1. The contribution of the electrostatic interaction (ΔE_{elstat}, 49.7%) is almost equal to that of the orbital interaction (ΔE_{orb}, 49.4%). The contribution of the dispersion energy correction (ΔE_{disp}, 0.9%) is negligible. There are eight major components to the total orbital interaction, which can be identified by relevant deformation density ($\Delta\rho$). While the plots of alpha-orbital deformation densities $\Delta\rho_{(1)-(8)}$ of $Cr(CO)_3$ and the shape of dominant interacting MOs are shown in Figure 5, those of beta-orbital deformation densities $\Delta\rho_{(6)-(8)}$ are shown in Figure S4. The most important contribution to the orbital interaction comes from $\Delta E_{orb(1)}$ (55.1%), which is attributed to Cr(s) → $(CO)_3$ π donation. For $\Delta\rho_{(1)}$, the LUMO of $(CO)_3$ and the Cr $4p_z$ AO receives the Cr 4s electron during the interaction, which can be described as a total interaction between the 2π* orbitals of $(CO)_3$ and the Cr $4p_z$ AO. The $\Delta E_{orb(n)}$ (n = 2−5) terms represent the backdonation of the Cr d electrons to the $(CO)_3$ 2π* orbitals, with a total contribution of 31.8%. The $\Delta E_{orb(n)}$ (n = 6−8) terms represent the σ-bonding interaction between the $(CO)_3$ 5σ orbital and the Cr 4s/4p AOs, accounting for 11.9%.

The above bonding analyses show a strong π-type bonding interaction between the Cr $4p_z$ AO and the $(CO)_3$ LUMO, which significantly contributes to keep the D_{3h} planar shape of

https://doi.org/10.1021/acs.jpca.4c01120
J. Phys. Chem. A 2024, 128, 3321−3328

Table 1. EDA-NOCV Results for $Cr(CO)_3$ ($^7A_2''$), Taking Cr and $(CO)_3$ as Interacting Fragments

energy term	assignment	energy (kcal/mol)	
ΔE_{int} [a]		−54.5	
ΔE_{Pauli}		400.0	
ΔE_{elstat} [b]		−225.8 (49.7%)	
ΔE_{orb} [b]		−224.5 (49.4%)	
ΔE_{disp} [b]		−4.3 (0.9%)	
spin		alpha	beta
$\Delta E_{orb(1)}$ [c]	Cr(s) → $(CO)_3$ π donation	−123.8 (55.1%)	
$\Delta E_{orb(2)}$ [c]	Cr(d) → $(CO)_3$ π donation	−25.9 (11.5%)	
$\Delta E_{orb(3)}$ [c]		−25.9 (11.5%)	
$\Delta E_{orb(4)}$ [c]		−9.9 (4.4%)	
$\Delta E_{orb(5)}$ [c]		−9.9 (4.4%)	
$\Delta E_{orb(6)}$ [c]	Cr(s) ← $(CO)_3$ σ donation	−3.0 (1.3%)	−4.9 (2.2%)
$\Delta E_{orb(7)}$ [c]	Cr(p) ← $(CO)_3$ σ donation	−2.8 (1.2%)	−6.7 (3.0%)
$\Delta E_{orb(8)}$ [c]		−2.8 (1.2%)	−6.7 (3.0%)
$\Delta E_{orb(rest)}$ [c]		0.0 (0.0%)	−2.2 (1.0%)

[a] $\Delta E_{int} = \Delta E_{Pauli} + \Delta E_{elstat} + \Delta E_{orb} + \Delta E_{disp}$. [b] The values in parentheses denote the contribution to the total attractive interactions $\Delta E_{elstat} + \Delta E_{orb} + \Delta E_{disp}$. [c] The values in the parentheses denote the percentage contribution to the total orbital interaction ΔE_{orb}.

$Cr(CO)_3$ ($^7A_2''$). The 3d orbitals of the Cr atom are split into three groups in the D_{3h} field, a_1', e'', and e'. The splitting energy $\Delta = E(e') - E(e'')$ is small (1.0 eV) and the electron pairing energy of d^5 configuration tends to be large, resulting in the high spin distribution of the half-full Cr 3d AOs according to the Hund rule.[40]

4. CONCLUSIONS

The present IR-VUV experimental spectra and theoretical simulations provide evidence for the formation of $Cr(CO)_3$ with an $^7A_2''$ highly excited state and a D_{3h} symmetry. The generation of this septet $Cr(CO)_3$ in a high-spin product channel is feasible both thermodynamically and kinetically. Electronic structure and bonding analyses show that the D_{3h} planar configuration of this highly excited $Cr(CO)_3$ is stabilized by a strong π-type bonding interaction between the Cr $4p_z$ AO and the LUMO of $(CO)_3$ and the high spin distribution of half-full Cr 3d AOs has special stability. This work stimulates further size-specific IR-VUV spectroscopic discoveries of various compounds with unconventional structures and properties.

■ ASSOCIATED CONTENT

Supporting Information

The Supporting Information is available free of charge at https://pubs.acs.org/doi/10.1021/acs.jpca.4c01120.

Comparison of the IR-VUV spectrum of $Cr(CO)_3$ with simulated vibrational spectra of different electronic states, structures of $Cr(CO)_n$ (n = 1 and 2), plots of the most important frontier MOs of $(CO)_3$, plots of beta-orbital deformation densities $\Delta\rho_{(6)-(8)}$ of $Cr(CO)_3$, calculated stretching modes and band positions of neutral $Cr(CO)_3$ with different electronic states, reaction energies of the $Cr(CO)_n$ (n = 1−3) formation, AO contributions of $Cr(CO)_3$, and Cartesian coordinates (PDF)

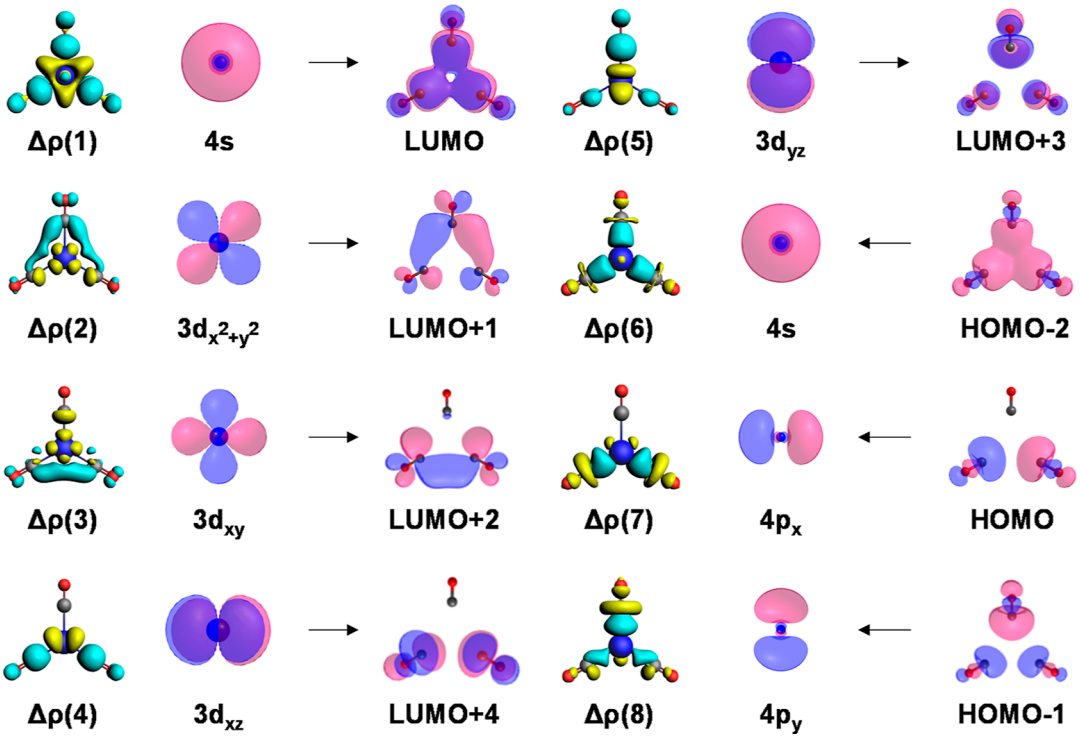

Figure 5. Deformation densities $\Delta\rho_{(1)-(8)}$ in the alpha orbitals of $Cr(CO)_3$ using Cr and $(CO)_3$ as interacting fragments and the shape of dominant interacting MOs of fragments. The isosurface values are set to 0.0015 for $\Delta\rho_{(1)-(3)}$ and 0.0005 for $\Delta\rho_{(4)-(8)}$. The charge flows from olive to cyan.

https://doi.org/10.1021/acs.jpca.4c01120
J. Phys. Chem. A 2024, 128, 3321−3328

AUTHOR INFORMATION

Corresponding Authors

Gang Li − *State Key Laboratory of Molecular Reaction Dynamics, Dalian Institute of Chemical Physics, Chinese Academy of Sciences, Dalian 116023, China;* orcid.org/0000-0001-5984-111X; Email: gli@dicp.ac.cn

Ling Jiang − *State Key Laboratory of Molecular Reaction Dynamics, Dalian Institute of Chemical Physics, Chinese Academy of Sciences, Dalian 116023, China; Hefei National Laboratory, Hefei 230088, China;* orcid.org/0000-0002-8485-8893; Email: ljiang@dicp.ac.cn

Authors

Tiantong Wang − *State Key Laboratory of Molecular Reaction Dynamics, Dalian Institute of Chemical Physics, Chinese Academy of Sciences, Dalian 116023, China; University of Chinese Academy of Sciences, Beijing 100049, China*

Zhaoyan Zhang − *State Key Laboratory of Molecular Reaction Dynamics, Dalian Institute of Chemical Physics, Chinese Academy of Sciences, Dalian 116023, China; University of Chinese Academy of Sciences, Beijing 100049, China*

Wenhui Yan − *State Key Laboratory of Molecular Reaction Dynamics, Dalian Institute of Chemical Physics, Chinese Academy of Sciences, Dalian 116023, China; University of Chinese Academy of Sciences, Beijing 100049, China*

Shuai Jiang − *State Key Laboratory of Molecular Reaction Dynamics, Dalian Institute of Chemical Physics, Chinese Academy of Sciences, Dalian 116023, China; University of Chinese Academy of Sciences, Beijing 100049, China*

Shangdong Li − *State Key Laboratory of Molecular Reaction Dynamics, Dalian Institute of Chemical Physics, Chinese Academy of Sciences, Dalian 116023, China; University of Chinese Academy of Sciences, Beijing 100049, China*

Jianxing Zhuang − *State Key Laboratory of Molecular Reaction Dynamics, Dalian Institute of Chemical Physics, Chinese Academy of Sciences, Dalian 116023, China; University of Chinese Academy of Sciences, Beijing 100049, China*

Hua Xie − *State Key Laboratory of Molecular Reaction Dynamics, Dalian Institute of Chemical Physics, Chinese Academy of Sciences, Dalian 116023, China;* orcid.org/0000-0003-2091-6457

Complete contact information is available at: https://pubs.acs.org/10.1021/acs.jpca.4c01120

Notes

The authors declare no competing financial interest.

ACKNOWLEDGMENTS

The authors gratefully acknowledge the Dalian Coherent Light Source (DCLS) for support and assistance. This work was supported by the National Natural Science Foundation of China (grant nos. 22125303, 92361302, 92061203, 22373102, 22103082, 22273101, 22288201, and 21327901), the National Key Research and Development Program of China (2021YFA1400501), the Youth Innovation Promotion Association of the Chinese Academy of Sciences (CAS) (2020187), the Innovation Program for Quantum Science and Technology (2021ZD0303304), the CAS (GJJSTD20220001), the Dalian Institute of Chemical Physics (DICP I202437), and the International Partnership Program of CAS (121421KYSB20170012).

REFERENCES

(1) Schoonover, J. R.; Strouse, G. F. Time-Resolved Vibrational Spectroscopy of Electronically Excited Inorganic Complexes in Solution. *Chem. Rev.* **1998**, *98*, 1335−1356.

(2) Juban, E. A.; Smeigh, A. L.; Monat, J. E.; McCusker, J. K. Ultrafast Dynamics of Ligand-Field Excited States. *Coord. Chem. Rev.* **2006**, *250*, 1783−1791.

(3) Butler, J. M.; George, M. W.; Schoonover, J. R.; Dattelbaum, D. M.; Meyer, T. J. Application of Transient Infrared and Near Infrared Spectroscopy to Transition Metal Complex Excited States and Intermediates. *Coord. Chem. Rev.* **2007**, *251*, 492−514.

(4) Mai, S.; Plasser, F.; Dorn, J.; Fumanal, M.; Daniel, C.; Gonzalez, L. Quantitative Wave Function Analysis for Excited States of Transition Metal Complexes. *Coord. Chem. Rev.* **2018**, *361*, 74−97.

(5) Jin, Y.; Zhang, Q.; Zhang, Y.; Duan, C. Electron Transfer in the Confined Environments of Metal-Organic Coordination Supramolecular Systems. *Chem. Soc. Rev.* **2020**, *49*, 5561−5600.

(6) Westermayr, J.; Marquetand, P. Machine Learning for Electronically Excited States of Molecules. *Chem. Rev.* **2021**, *121*, 9873−9926.

(7) Parshall, G. W. Organometallic Chemistry in Homogeneous Catalysis. *Science* **1980**, *208*, 1221−1224.

(8) Gray, H. B.; Maverick, A. W. Solar Chemistry of Metal-Complexes. *Science* **1981**, *214*, 1201−1205.

(9) Heyduk, A. F.; Nocera, D. G. Hydrogen Produced from Hydrohalic Acid Solutions by a Two-Electron Mixed-Valence Photocatalyst. *Science* **2001**, *293*, 1639−1641.

(10) Esswein, A. J.; Nocera, D. G. Hydrogen Production by Molecular Photocatalysis. *Chem. Rev.* **2007**, *107*, 4022−4047.

(11) Labinger, J. A.; Bercaw, J. E. Understanding and Exploiting C-H Bond Activation. *Nature* **2002**, *417*, 507−514.

(12) Jay, R. M.; Banerjee, A.; Leitner, T.; Wang, R.-P.; Harich, J.; Stefanuik, R.; Wikmark, H.; Coates, M. R. V.; Beale, E.; Kabanova, V.; et al. Tracking C-H Activation with Orbital Resolution. *Science* **2023**, *380*, 955−960.

(13) Kunnus, K.; Rajkovic, I.; Schreck, S.; Quevedo, W.; Eckert, S.; Beye, M.; Suljoti, E.; Weniger, C.; Kalus, C.; Grübel, S.; et al. A Setup for Resonant Inelastic Soft X-Ray Scattering on Liquids at Free Electron Laser Light Sources. *Rev. Sci. Instrum.* **2012**, *83*, 123109.

(14) Wernet, P.; Kunnus, K.; Josefsson, I.; Rajkovic, I.; Quevedo, W.; Beye, M.; Schreck, S.; Grübel, S.; Scholz, M.; Nordlund, D.; et al. Orbital-Specific Mapping of the Ligand Exchange Dynamics of $Fe(CO)_5$ in Solution. *Nature* **2015**, *520*, 78−81.

(15) Cordones, A. A.; Lee, J. H.; Hong, K.; Cho, H.; Garg, K.; Boggio-Pasqua, M.; Rack, J. J.; Huse, N.; Schoenlein, R. W.; Kim, T. K. Transient Metal-Centered States Mediate Isomerization of a Photochromic Rutheniumsulfoxide Complex. *Nat. Commun.* **2018**, *9*, 1989.

(16) Bartlett, S. A.; Besley, N. A.; Dent, A. J.; Diaz-Moreno, S.; Evans, J.; Hamilton, M. L.; Hanson-Heine, M. W. D.; Horvath, R.; Manici, V.; Sun, X.-Z.; et al. Monitoring the Formation and Reactivity of Organometallic Alkane and Fluoroalkane Complexes with Silanes and Xe Using Time-Resolved X-Ray Absorption Fine Structure Spectroscopy. *J. Am. Chem. Soc.* **2019**, *141*, 11471−11480.

(17) Bistoni, G.; Rampino, S.; Scafuri, N.; Ciancaleoni, G.; Zuccaccia, D.; Belpassi, L.; Tarantelli, F. How π Back-Donation Quantitatively Controls the CO Stretching Response in Classical and Non-Classical Metal Carbonyl Complexes. *Chem. Sci.* **2016**, *7*, 1174−1184.

(18) Turner, J. J.; George, M. W.; Poliakoff, M.; Perutz, R. N. Photochemistry of Transition Metal Carbonyls. *Chem. Soc. Rev.* **2022**, *51*, 5300−5329.

(19) Fielicke, A. Probing the Binding and Activation of Small Molecules by Gas-Phase Transition Metal Clusters via IR Spectroscopy. *Chem. Soc. Rev.* **2023**, *52*, 3778−3841.

(20) Lomont, J. P.; Nguyen, S. C.; Harris, C. B. Ultrafast Infrared Studies of the Role of Spin States in Organometallic Reaction Dynamics. *Acc. Chem. Res.* **2014**, *47*, 1634−1642.
(21) Reinhard, M.; Auböck, G.; Besley, N. A.; Clark, I. P.; Greetham, G. M.; Hanson-Heine, M. W. D.; Horvath, R.; Murphy, T. S.; Penfold, T. J.; Towrie, M.; et al. Photoaquation Mechanism of Hexacyanoferrate(II) Ions: Ultrafast 2D UV and Transient Visible and IR Spectroscopies. *J. Am. Chem. Soc.* **2017**, *139*, 7335−7347.
(22) Cole-Filipiak, N. C.; Troß, J.; Schrader, P.; McCaslin, L. M.; Ramasesha, K. Ultraviolet Photodissociation of Gas-Phase Iron Pentacarbonyl Probed with Ultrafast Infrared Spectroscopy. *J. Chem. Phys.* **2021**, *154*, 134308.
(23) Macoas, E. M. S.; Mustalahti, S.; Myllyperkio, P.; Kunttu, H.; Pettersson, M. Role of Vibrational Dynamics in Electronic Relaxation of $Cr(acac)_3$. *J. Phys. Chem. A* **2015**, *119*, 2727−2734.
(24) Snee, P. T.; Payne, C. K.; Mebane, S. D.; Kotz, K. T.; Harris, C. B. Dynamics of Photosubstitution Reactions of $Fe(CO)_5$: An Ultrafast Infrared Study of High Spin Reactivity. *J. Am. Chem. Soc.* **2001**, *123*, 6909−6915.
(25) Rosillo, M.; Domínguez, G.; Pérez-Castells, J. Chromium Arene Complexes in Organic Synthesis. *Chem. Soc. Rev.* **2007**, *36*, 1589−1604.
(26) Zhao, W.; Huang, X.; Zhan, Y.; Zhang, Q.; Li, D.; Zhang, Y.; Kong, L.; Peng, B. Dearomative Dual Functionalization of Aryl Iodanes. *Angew. Chem., Int. Ed.* **2019**, *58*, 17210−17214.
(27) Wang, M.-Y.; Wu, C.-J.; Zeng, W.-L.; Jiang, X.; Li, W. Dearomative Aminocarbonylation of Arenes via Bifunctional Coordination to Chromium. *Angew. Chem., Int. Ed.* **2022**, *61*, No. e202210312.
(28) Bolm, C.; Muñiz, K. Planar Chiral Arene Chromium(0) Complexes: Potential Ligands for Asymmetric Catalysis. *Chem. Soc. Rev.* **1999**, *28*, 51−59.
(29) Li, K.; Wu, W.-Q.; Lin, Y.; Shi, H. Asymmetric Hydrogenation of 1,1-Diarylethylenes and Benzophenones Through a Relay Strategy. *Nat. Commun.* **2023**, *14*, 2170.
(30) Qiu, J.-Y.; Zeng, W.-L.; Xie, H.; Wang, M.-Y.; Li, W. Chemoselective 1,2-Reduction and Regiodivergent Deuteration of Chromium-Bound Arenes. *Angew. Chem., Int. Ed.* **2023**, *62*, No. e202218961.
(31) Dötz, K. H.; Stendel, J. Fischer Carbene Complexes in Organic Synthesis: Metal-Assisted and Metal-Templated Reactions. *Chem. Rev.* **2009**, *109*, 3227−3274.
(32) Türker, L.; Gümüş, S. *Ab initio* and DFT Studies on Certain η^6-Anthraquinone -$Cr(CO)_3$ Complexes. *Polycycl. Aromat. Compd.* **2008**, *28*, 181−192.
(33) Seder, T. A.; Church, S. P.; Weitz, E. Wavelength Dependence of Excimer Laser Photolysis of $Cr(CO)_6$ in the Gas Phase. A Study of the Infrared Spectroscopy and Reactions of the $Cr(CO)_x$ (x = 5, 4, 3, 2) Fragments. *J. Am. Chem. Soc.* **1986**, *108*, 4721−4728.
(34) Perutz, R. N.; Turner, J. J. Photochemistry of the Group 6 Hexacarbonyls in Low-Temperature Matrixes. IV. Tetracarbonylmolybdenum and Tricarbonylmolybdenum. *J. Am. Chem. Soc.* **1975**, *97*, 4800−4804.
(35) Andrews, L.; Zhou, M.; Gutsev, G. L.; Wang, X. Reactions of Laser-Ablated Chromium Atoms, Cations, and Electrons with CO in Excess Argon and Neon: Infrared Spectra and Density Functional Calculations on Neutral and Charged Unsaturated Chromium Carbonyls. *J. Phys. Chem. A* **2003**, *107*, 561−569.
(36) Kim, J.; Kim, T. K.; Kim, J.; Lee, Y. S.; Ihee, H. Density Functional and Ab Initio Study of $Cr(CO)_n$ (n = 1−6) Complexes. *J. Phys. Chem. A* **2007**, *111*, 4697−4710.
(37) Trushin, S. A.; Kosma, K.; Fuß, W.; Schmid, W. E. Wavelength-Independent Ultrafast Dynamics and Coherent Oscillation of a Metal-Carbon Stretch Vibration in Photodissociation of $Cr(CO)_6$ in the Region of 270−345 nm. *Chem. Phys.* **2008**, *347*, 309−323.
(38) Kim, J.; Kim, J.; Ihee, H. Multireference Ab Initio Study of the Ground and Low-Lying Excited States of $Cr(CO)_2$ and $Cr(CO)_3$. *J. Phys. Chem. A* **2013**, *117*, 3861−3868.
(39) Bengali, A. A.; Casey, S. M.; Cheng, C. L.; Dick, J. P.; Fenn, P. T.; Villalta, P. W.; Leopold, D. G. Negative Ion Photoelectron Spectroscopy of Coordinatively Unsaturated Group VI Metal Carbonyls of chromium, molybdenum and tungsten: $Cr(CO)_3$, $Mo(CO)_3$, and $W(CO)_3$. *J. Am. Chem. Soc.* **1992**, *114*, 5257−5268.
(40) Zhou, M. F.; Andrews, L.; Bauschlicher, C. W. Spectroscopic and Theoretical Investigations of Vibrational Frequencies in Binary Unsaturated Transition-Metal Carbonyl Cations, Neutrals, and Anions. *Chem. Rev.* **2001**, *101*, 1931−1962.
(41) Li, G.; Wang, C.; Li, Q. M.; Zheng, H. J.; Wang, T. T.; Yu, Y.; Su, M. Z.; Yang, D.; Shi, L.; Yang, J. Y.; et al. Infrared + Vacuum Ultraviolet Two-Color Ionization Spectroscopy of Neutral Metal Complexes Based on a Tunable Vacuum Ultraviolet Free-Electron Laser. *Rev. Sci. Instrum.* **2020**, *91*, 034103.
(42) Zhang, B. B.; Yu, Y.; Zhang, Z. J.; Zhang, Y. Y.; Jiang, S. K.; Li, Q. M.; Yang, S.; Hu, H. S.; Zhang, W. Q.; Dai, D. X.; et al. Infrared Spectroscopy of Neutral Water Dimer Based on a Tunable Vacuum Ultraviolet Free Electron Laser. *J. Phys. Chem. Lett.* **2020**, *11*, 851−855.
(43) Li, G.; Wang, C.; Zheng, H.-j.; Wang, T.-t.; Xie, H.; Yang, X.-m.; Jiang, L. Infrared Spectroscopy of Neutral Clusters Based on a Vacuum Ultraviolet Free Electron Laser. *Chin. J. Chem. Phys.* **2021**, *34*, 51−60.
(44) Frisch, M. J.; Trucks, G. W.; Schlegel, H. B.; Scuseria, G. E.; Robb, M. A.; Cheeseman, J. R.; Scalmani, G.; Barone, V.; Petersson, G. A.; Nakatsuji, H.; et al. *Gaussian 16*. Rev. B.01; Gaussian, Inc.: Wallingford, CT, 2016.
(45) te Velde, G.; Bickelhaupt, F. M.; Baerends, E. J.; Guerra, C. F.; Van Gisbergen, S. J. A.; Snijders, J. G.; Ziegler, T. Chemistry with ADF. *J. Comput. Chem.* **2001**, *22*, 931−967.
(46) Baerends, E. J.; Ziegler, T.; Autschbach, J.; Bashford, D.; Bérces, A.; Bickelhaupt, F. M.; Bo, C.; Boerrigter, P. M.; Cavallo, L.; Chong, D. P.; et al. *ADF2023, SCM, Theoretical Chemistry*; Vrije Universiteit: Amsterdam, The Netherlands, 2023.
(47) Mitoraj, M. P.; Michalak, A.; Ziegler, T. A Combined Charge and Energy Decomposition Scheme for Bond Analysis. *J. Chem. Theory Comput.* **2009**, *5*, 962−975.
(48) Savin, A.; Nesper, R.; Wengert, S.; Fassler, T. F. ELF: The Electron Localization Function. *Angew. Chem., Int. Ed.* **1997**, *36*, 1808−1832.
(49) Kohout, M.; Wagner, F. R.; Grin, Y. Electron Localization Function for Transition-Metal Compounds. *Theor. Chem. Acc.* **2002**, *108*, 150−156.
(50) Lu, T.; Chen, F. Multiwfn: A Multifunctional Wavefunction Analyzer. *J. Comput. Chem.* **2012**, *33*, 580−592.
(51) Duncan, M. A. Invited Review Article: Laser vaporization cluster sources. *Rev. Sci. Instrum.* **2012**, *83*, 041101.
(52) Pilme, J.; Silvi, B.; Alikhani, M. E. Structure and Stability of M-CO, M = First-Transition-Row Metal: An Application of Density Functional Theory and Topological Approaches. *J. Phys. Chem. A* **2003**, *107*, 4506−4514.
(53) Zimmermann, J.; Zeug, A.; Röder, B. A Generalization of the Jablonski Diagram to Account for Polarization and Anisotropy Effects in Time-Resolved Experiments. *Phys. Chem. Chem. Phys.* **2003**, *5*, 2964−2969.
(54) Feng, G.; Zhang, G.-Q.; Ding, D. Design of Superior Phototheranostic Agents Guided by Jablonski Diagrams. *Chem. Soc. Rev.* **2020**, *49*, 8179−8234.
(55) Zhang, Y.; Liu, H.; Weng, Y. Theoretical and Experimental Investigation of the Electronic Propensity Rule: A Linear Relationship Between Radiative and Nonradiative Decay Rates of Molecules. *J. Phys. Chem. Lett.* **2023**, *14*, 4151−4157.
(56) Delor, M.; Scattergood, P. A.; Sazanovich, I. V.; Parker, A. W.; Greetham, G. M.; Meijer, A. J. H. M.; Towrie, M.; Weinstein, J. A. Toward Control of Electron Transfer in Donor-Acceptor Molecules by Bond-Specific Infrared Excitation. *Science* **2014**, *346*, 1492−1495.
(57) Zhang, W.; Gaffney, K. J. Mechanistic Studies of Photoinduced Spin Crossover and Electron Transfer in Inorganic Complexes. *Acc. Chem. Res.* **2015**, *48*, 1140−1148.

https://doi.org/10.1021/acs.jpca.4c01120
J. Phys. Chem. A 2024, 128, 3321−3328

(58) Penfold, T. J.; Gindensperger, E.; Daniel, C.; Marian, C. M. Spin-Vibronic Mechanism for Intersystem Crossing. *Chem. Rev.* **2018**, *118*, 6975−7025.

https://doi.org/10.1021/acs.jpca.4c01120
J. Phys. Chem. A 2024, 128, 3321−3328